

Microstructure and Mechanical Properties of Dissimilar Welded Ti₃Al/Ni-Based Superalloy Joint Using a Ni-Cu Filler Alloy

BING-QING CHEN, HUA-PING XIONG, SHAO-QING GUO, BING-BING SUN,
BO CHEN, and SI-YI TANG

Dissimilar welding of a Ti₃Al-based alloy and a Ni-based superalloy (Inconel 718) was successfully carried out using gas tungsten arc welding technology in this study. With a Ni-Cu alloy as filler material, sound joints have been obtained. The microstructure evolution along the cross section of the dissimilar joint has been revealed based on the results of scanning electron microscopy and X-ray energy dispersive spectroscopy as well as X-ray diffractometer. It is found that the weld/Ti₃Al interface is composed of Ti₂AlNb matrix dissolved with Ni and Cu, Al(Cu, Ni)₂Ti, (Cu, Ni)₂Ti, (Nb, Ti) solid solution, and so on. The weld and In718/weld interface mainly consist of (Cu, Ni) solid solutions. The weld exhibits higher microhardness than the two base materials. The average room-temperature tensile strength of the joints reaches 242 MPa and up to 73.6 pct of the value can be maintained at 873 K (600 °C). The brittle intermetallic phase of Ti₂AlNb matrix dissolved with Ni and Cu at the weld/Ti₃Al interface is the weak link of the joint.

DOI: 10.1007/s11661-014-2652-z

© The Minerals, Metals & Materials Society and ASM International 2014

I. INTRODUCTION

INTERMETALLIC compounds have attracted a great deal of attention because they have low densities and maintain high strength at elevated temperatures. One type of such intermetallic alloys, Ti₃Al-based alloy, is of great interest due to its desirable properties such as high specific modulus and good creep resistance, implying excellent performance in aerospace field.^[1,2] Obviously, in order to realize the practical engineering applications of Ti₃Al-based alloy, joining Ti₃Al to other materials such as Ni-based superalloy is an unavoidable and extremely important processing technology.

Fusion welding is one of the most widely used methods for the joining of metallic materials. In past decades, a number of studies have been performed on the weldability of Ti₃Al-based alloy with fusion welding processes.^[3] David *et al.* indicated that Ti-24Al-11Nb (at. pct) alloy showed excellent resistance to solidification cracking but a tendency to crack during cooling (solid-state cracking) when using electron beam and gas tungsten arc welding technologies.^[4] Baeslack *et al.* characterized the phase transformations resulting from fusion and solid-state processing of Ti-26Al-11Nb (at. pct) alloy.^[5] It is pointed out in the above two reports that cooling rate has a profound effect on the microstructures and properties of Ti₃Al welds. In Liu *et al.*'s research, it was found that

with proper preheating process, the solid-state crack sensitivity of the Ti₃Al joint was effectively reduced, and post-weld heat treatments could improve the microstructures of the weld as well as the heat-affected zone.^[6] Wu *et al.* indicated that the room-temperature tensile strength of the Ti-24Al-17Nb (at. pct) joint using laser beam welding was equal to that of the base material^[7] and Lei *et al.* investigated the average tensile strength of the laser-welded Ti-22Al-27Nb (at. pct) joints at 923 K (650 °C), which was tested to be about 733 MPa.^[8] With respect to dissimilar welding between Ti₃Al-based alloy and other materials, studies were also carried out with fusion welding processes. Feng *et al.* investigated the interfacial microstructure and mechanical properties of the dissimilar joint of Ti₃Al and TC4 alloys welded by electron beam welding process, and the highest tensile strength of the joints could reach almost 92 pct of that of the Ti₃Al-based alloy.^[9] The joining of Ti-22Al-25Nb and TC11 alloys was also carried out using electron beam welding technique, the room-temperature tensile strength of the joint was higher than that of the TC11 base alloy, and the impact toughness was found to be about 42 pct of that of the TC11 alloy.^[10] These investigations were primarily focused on welding of Ti₃Al to Ti-based alloys.

In fact, the dissimilar joining of Ti₃Al-based alloy to Ni-based superalloy is more attractive for engineering applications because of its high-temperature service potential as well as the weight reduction effects. For example, Ti₃Al-based alloy is regarded as the suitable material of the outer casing of advanced aeroengine compressor and thus the connection between the outer casing and the mounting edge usually made of Inconel 718 superalloy needs the dissimilar joining technology. However, the corresponding research work is lacking.

BING-QING CHEN, SHAO-QING GUO, and BO CHEN, Senior Engineers, HUA-PING XIONG, Professor, BING-BING SUN and SI-YI TANG, Engineers, are with the 3D Printing Research and Engineering Technology Center, Beijing Institute of Aeronautical Materials, Beijing 100095, P. R. China. Contact e-mail: xionghp69@163.com

Manuscript submitted May 12, 2014.

Article published online November 18, 2014

Actually, it has been recognized that the joining of Ti₃Al-based alloy to Ni-based superalloy is extremely difficult because of the following reasons^[11–13]: (1) The dissolution enthalpy of Ti in liquid Ni solvent is -170 kJ/mol^[14] and according to the Ti-Ni binary alloy phase diagram,^[15] kinds of Ti-Ni intermetallics such as Ti₂Ni, TiNi, and TiNi₃ could form, indicating the high affinity of the two elements. This could result in the strong tendency to form brittle intermetallic phases across the joint interface, which is detrimental to the mechanical properties of the joint and could even induce cracking.^[16] (2) Composition becomes a parameter that varies over a wide range across the weld pool. Consequently, there does not exist a single liquidus isotherm that defines the solid-liquid interface as it does in similar metals welding. (3) Thermo-physical properties of the two base materials are quite different. For example, the thermal diffusivity and thermal expansion coefficient of Ni-based superalloy are much higher than those of Ti₃Al-based alloy (roughly twice), which could influence the heat transfer during the welding process and induce large residual stress in the joint. The above three problems probably encountered during welding make the joining of Ti₃Al to Ni-based superalloy a great challenge.

In previous research, several filler materials were tried to join the two alloys. When welded with Nicochrome, though the weld showed good metallurgical compatibility with the Ni-based superalloy, the joint cracked at the interface between the weld and Ti₃Al base alloy immediately after welding. Other filler materials adopted showed similar results: The joints cracked at the In718/weld interface or weld/Ti₃Al interface during or after welding. In this study, the working temperature of the Ti₃Al/Ni-based superalloy joint expected was 873 K to 923 K (600 °C to 650 °C), so an attempt was made to join the two alloys by gas tungsten arc (GTA) welding technology using a Ni-Cu alloy as filler material. It is known that Ni-Cu alloy owns good metallurgical compatibility with Ni-based superalloy and its superior ductility is helpful to relieve the residual stress of the dissimilar joint through plastic deformation. The microstructure and mechanical properties of the joints were investigated.

II. EXPERIMENTAL PROCEDURES

The Ti₃Al-based alloy used for GTA welding is Ti-24Al-15Nb-1Mo (at. pct) composed of $\alpha_2 + O$ (Ti₂AlNb) + B2 three phase equiaxial grains,^[17] which was prepared by the following steps: vacuum-consumable electrode arc melting, breaking down in the β /B2 phase fields, forging and rolling in the $\alpha_2 + B2$ phase field, and heat treating at 1253 K (980 °C) for 1 h followed by cooling in air. The other base material to be joined in this experiment is Inconel 718 (In718) superalloy, with long-term working temperature of 973 K (700 °C). The nominal chemical composition of In718 is primarily (wt pct) 50.0~55.0 Ni, 17.0~21.0 Cr, 2.80~3.30 Mo, 4.75~5.50 Nb, 0.75~1.15 Ti, 0.30~0.70 Al, and balance Fe.

Rectangular plates of 2.8 mm in thickness were machined from the Ti-24Al-15Nb-1Mo and In718 alloys. The filler material is a Ni-Cu solid solution alloy with 2 mm diameter, whose chemical composition is primarily (wt pct) 62.0~68.0 Ni, ≤ 1.0 Ti, ≤ 0.75 Al, ≤ 2.5 Fe, ≤ 4.0 Mn, ≤ 1.0 Si, and balance Cu. Before welding, the base alloys to be joined were preheated to 523 K (250 °C) in an air heat treatment furnace. Then GTA welding of Ti-24Al-15Nb-1Mo and In718 alloys was carried out using the following parameters: welding speed 90 mm/min, current 60 A DC, and voltage 14 V. To prevent oxidation during the welding processes, flowing argon shielding was applied at flow rates of 15, 20, and 8 L/minute to the top, tail, and bottom surfaces of the weld bead, respectively. The as-welded samples were subjected to furnace cooling with a cooling rate of 0.02 K/second from about 523 K (250 °C) to room temperature.

The as-welded specimens were sectioned transversely to the welding direction. The joint microstructures were observed by scanning electron microscopy (SEM; CS-3400) and the corresponding chemical composition analysis was performed using an X-ray energy dispersive spectroscopy (EDS). Microhardness values at various positions of the cross section of the joint were measured using a Vickers hardness tester (450-SVD) with a load of 200 g and loading time of 15 s. At least 5 indentations were performed at the same region. Transverse samples were machined from the as-welded plates and they were subjected to tensile tests at room temperature and at 873 K (600 °C). The fractured surfaces of the joints were also inspected by SEM and EDS. The phase constitution of the weld/Ti₃Al interface was identified using an X-ray diffractometer (XRD) by polishing the fractured surface of the joint subjected to the tensile test off 50-60 μm .

III. RESULTS AND DISCUSSION

The typical appearance of the as-welded Ti₃Al/In718 joint is shown in Figure 1, indicating the base alloys have been well wetted by the filler material and the welding bead morphology is relatively uniform. No macrocrack or incomplete fusion is found in the joint. Figure 2 displays the back-scattered electron (BSE) image of the cross section of the Ti₃Al/In718 joint. In the present research, with the Ni-Cu alloy as filler material, sound joints have been formed and no interface cracks are visible. It is demonstrated in the picture that a full penetration weld has been gained and the fusion zone with a width of about 3.5 mm is clearly distinguished from the base alloys.

Microstructure evolution along the cross section of the joint is characterized in detail in Figure 3. As shown in Figures 3(a) and (b), the weld/Ti₃Al interface shows a very complicated feature. The interface exhibits a layered microstructure and is constituted of three characteristic layers labeled as “A,” “B,” and “C” from Ti₃Al base material to the weld. Layer “A” is adjacent to the Ti₃Al base alloy and possesses the thickness of about 50 to 80 μm . This layer contains a large number of bright precipitates embedded in the light gray matrix

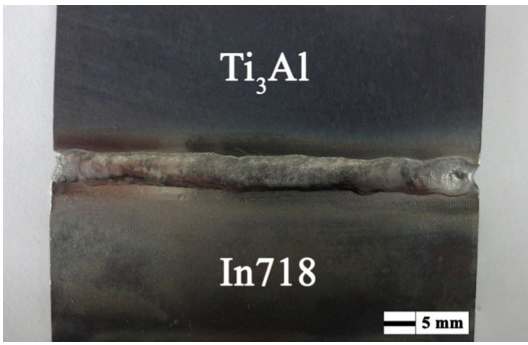


Fig. 1—Appearance of the as-welded Ti₃Al/In718 joint.

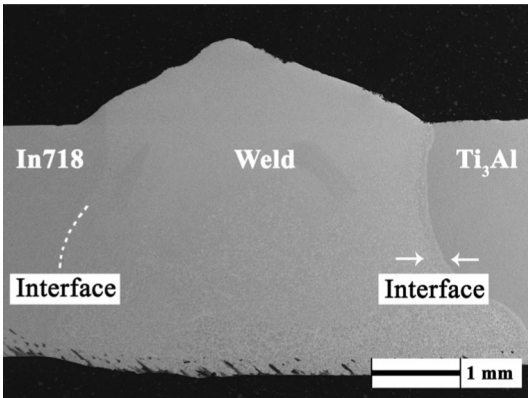


Fig. 2—BSE image of the cross section of the Ti₃Al/In718 joint.

composed of columnar dendrites. Layer “B” with about 100 μm in thickness consists of crystalline grains with various contrasts, shapes as well as dimensions. This layer also contains lots of high bright precipitates in the form of particle and strip. Layer “C” is next to the weld, with about 170 μm thickness, which mainly consists of coarse dendrites growing from the weld and fine crystals.

The representative phases at the weld/Ti₃Al interface are marked by white lines and numerals in Figures 3(a) and (b). The corresponding compositions obtained by EDS are presented in Table I. This table also shows the presumed phases by referring to the binary and ternary alloy phase diagrams. During welding, elements from the base materials and filler material diffused to each other under the driving force of concentration gradient. According to the composition analysis results, the main component of the light gray matrix (labeled “1” in Figure 3(a) in layer “A” is verified to be Ti₂AlNb dissolved with Ni and Cu, as this layer is just next to the Ti₃Al base alloy. It appears that during the welding process, elements of Ni and Cu diffused from the Ni-Cu filler alloy and dissolved into the surface layer of the Ti₃Al base alloy.

In layer “B,” during the fusion process, a liquid mixture of elements from Ti₃Al and the Ni-Cu alloy was formed. Then Ti, Al, Cu, and Ni reacted and solidified as Al(Cu, Ni)₂Ti and (Cu, Ni)₂Ti phases (labeled “2” and “3” in Figure 3a, respectively), as deduced from the composition analysis results and the Al-Cu-Ti ternary alloy phase diagram.^[18] Figure 4 shows the XRD pattern of the weld/Ti₃Al interface obtained by

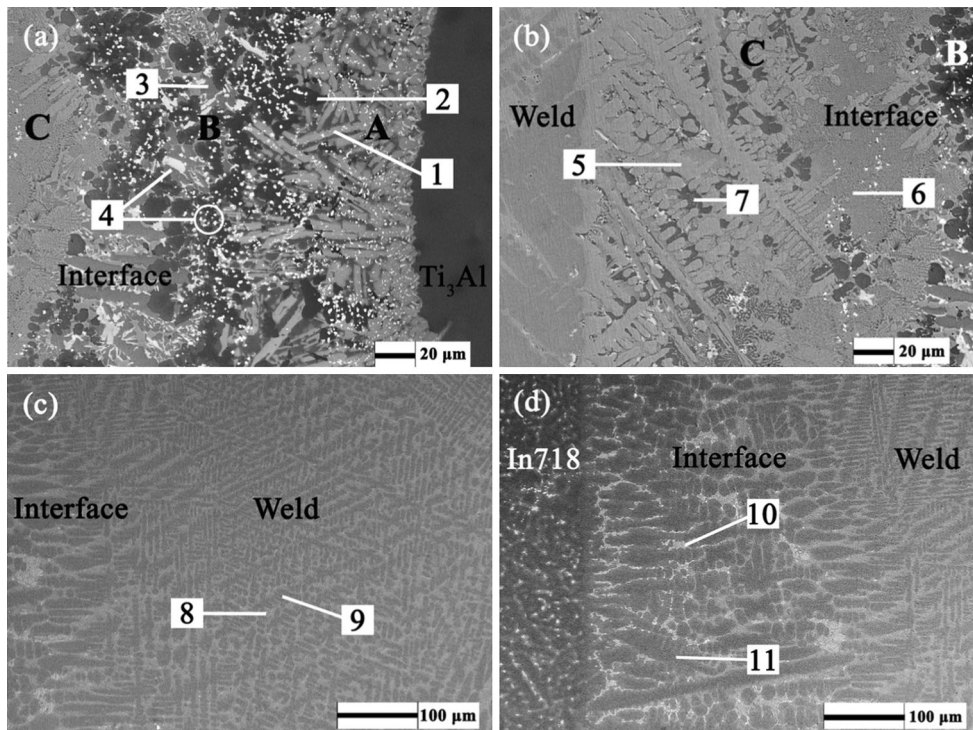


Fig. 3—Microstructure evolution along the cross section of the Ti₃Al/In718 joint. (a) Weld/Ti₃Al interface close to the Ti₃Al base alloy. (b) Weld/Ti₃Al interface close to the weld. (c) Fusion weld. (d) In718/weld interface.

Table I. Compositions of the Representative Phases and the Corresponding Deduced Phases

Position	Composition (Atomic Percent)								Deduced Phase
	Ti	Ni	Cu	Al	Nb	Fe	Cr	Mo	
1	39.6	13.7	17.9	12.3	15.5	0.6	0.4	—	Ti ₂ AlNb matrix dissolved with Ni and Cu
2	26.1	26.6	28.1	17.3	1.0	0.7	0.2	—	Al(Cu, Ni) ₂ Ti
3	31.6	19.6	46.1	0.8	1.4	0.5	—	—	(Cu, Ni) ₂ Ti
4	24.0	14.3	12.1	5.1	43.0	0.6	0.9	—	(Nb, Ti) solid solution dissolved with Cu, Ni, and Al
5	5.1	13.5	75.9	3.2	0.7	0.8	0.8	—	(Cu, Ni) solid solution
6	14.4	31.3	42.9	7.7	2.1	1.1	0.5	—	(Cu, Ni)-Ti compound
7	18.1	37.1	30.3	9.5	2.7	1.5	0.8	—	(Cu, Ni)-Ti compound
8	8.1	35.4	31.4	2.2	6.2	6.9	7.9	1.9	(Cu, Ni) solid solution dissolved with Fe, Cr, Nb, and Ti
9	7.2	37.1	40.7	2.8	1.7	5.4	4.6	0.5	(Cu, Ni) solid solution dissolved with Fe and Ti
10	8.5	38.6	24.9	1.9	7.8	8.9	9.4	—	(Cu, Ni) solid solution dissolved with Fe, Cr, Nb, and Ti
11	5.9	42.7	27.9	2.1	1.8	9.6	9.0	1.0	(Cu, Ni) solid solution dissolved with Fe, Cr, and Ti

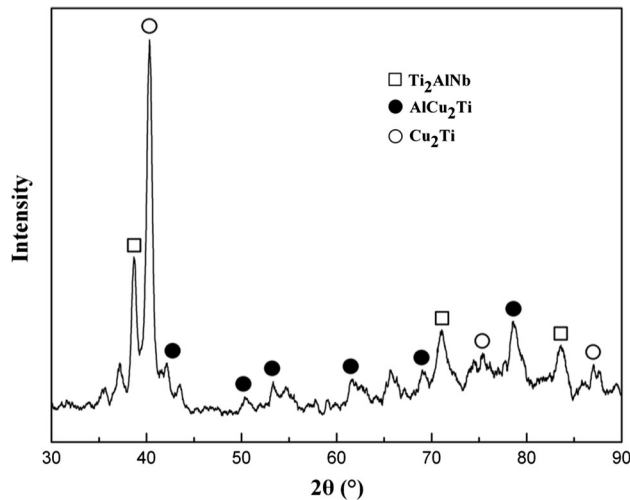


Fig. 4—XRD pattern of the weld/Ti₃Al interface 50 to 60 μm below the fractured surface.

polishing the fractured surface of the joint subjected to tensile test (presented below) off 50 to 60 μm, and it is assumed from Figure 3(a) that in this examined region, the phases in both layer “A” and layer “B” can be detected. As shown in Figure 4, the peaks corresponding to AlCu₂Ti, Cu₂Ti, and Ti₂AlNb phases are observed.

These phases were also identified as the reaction products in the joints in several references.^[19] For example, Lee *et al.* classified TiCu₂ and Ti(Cu, Ni) as the major phases near the fracture surfaces of infrared brazed γ-TiAl joints,^[20] Shiu *et al.* reported the formation of AlCu₂Ti and AlCuTi at the interface between BAG-8 and TiAl when joining TiAl intermetallic alloy using BAG-8 braze alloy,^[21] and Tetsui pointed out that AlM₂Ti type hard B2 intermetallics was formed inside brazed joints and at the boundaries to TiAl as a result of reactions of TiAl with Cu, Ni, or Au from the brazing filler.^[21,22] According to the Al-Cu-Ti ternary alloy phase diagram,^[18] there is a binary eutectic reaction at 1293 K (1020 °C) which is $L = \text{AlCu}_2\text{Ti} + (\text{Cu})$ and a transition reaction at 1173 K (900 °C) which

is $L + (\text{Cu}) = \text{AlCu}_2\text{Ti} + \text{Cu}_2\text{Ti}$. So, in this study, it is not strange that Al(Cu, Ni)₂Ti and (Cu, Ni)₂Ti phases are observed at the weld/Ti₃Al interface. At the same time, (Nb, Ti) solid solutions precipitated in both layer “A” and layer “B” (labeled “4” in Figure 3(a)) as the shiny particles and strips, dissolved with Cu, Ni, and Al.

For layer “C,” as adjacent to the weld, the dendritic crystals growing from the weld are classified as (Cu, Ni) solid solution (labeled “5” in Figure 3(b)). The crystals tended to be coarse due to the relatively slower cooling rate in this region. Ti, Nb, and Al from the Ti₃Al base material dissolved into this layer and thus at the interface between (Cu, Ni) dendrites and layer “B,” (Cu, Ni)-Ti compounds (labeled “6” in Figure 3(b)) were generated. According to the composition analysis results, the interdendritic phase showing dark contrast is also identified as (Cu, Ni)-Ti compound (labeled “7” in Figure 3(b)).

The microstructure of the weld is displayed in Figure 3(c). It shows a well-defined dendritic microstructure with small arm spacings and interdendritic regions, which is a Ni-Cu alloy (labeled “8” and “9” in Figure 3(c)) with several solid solution elements from the base materials.

As shown in Figure 3(d), the In718/weld interface indicates good metallurgical combination and there is a distinct boundary between the weld and base alloy. It is evident from the composition analysis results that the In718/weld interface is (Cu, Ni) solid solution dissolved with Fe, Cr, Nb, and Ti. The crystals exhibit coarser characteristic than the weld. Furthermore, compared with the weld, this interface has a lower Cu content and is richer in Fe and Cr as it is closer to the In718 base alloy. It should be pointed out that in the fusion weld and at the In718/weld interface, the microstructures are quite complicated. They are monotonously (Cu, Ni) solid solutions, but dissolved with two, three, or four elements of Ti, Nb, Fe, and Cr.

Variations of microhardness along the cross section of the joint are shown in Figure 5. For the weld/Ti₃Al interface, it is observed that layer “A” shows a sudden and great increase in microhardness compared to the Ti₃Al base alloy. And the value drops gradually as the distance from Ti₃Al increases. The high hardness value

at the interface is attributed to the microstructure which contains lots of intermetallic compounds. The whole weld exhibits higher microhardness than the two base

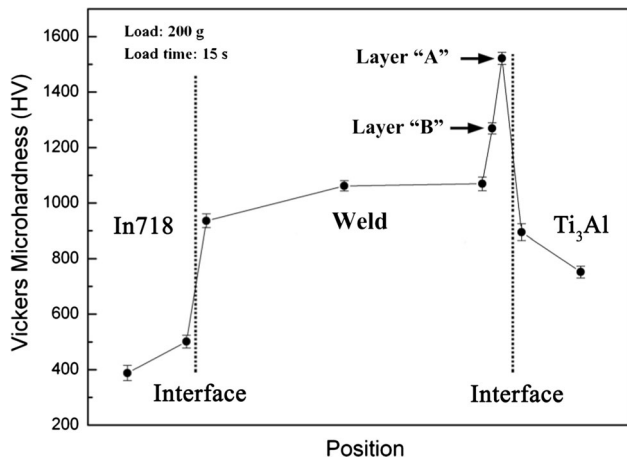


Fig. 5—Microhardness profile along the cross section of the $Ti_3Al/In718$ joint.

Table II. Tensile Strength of the $Ti_3Al/In718$ Joints

Tensile Strength (MPa)	1	2	3	4	5	Average Value (MPa)
Room temperature	207	191	273	256	285	242
873 K (600 °C)	201	187	147	—	—	178

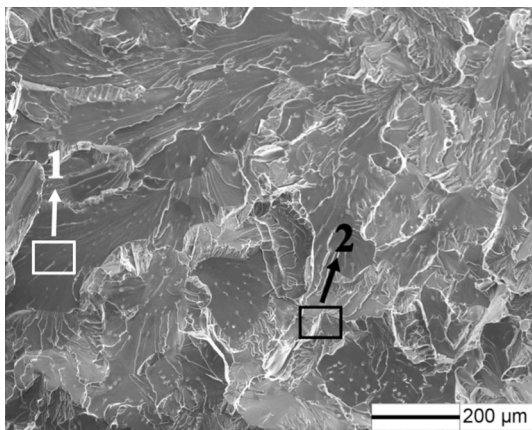


Fig. 6—Morphology of fractured surface of the $Ti_3Al/In718$ joint subjected to room-temperature tensile test.

materials. During welding, the weld metal was solid dissolved with various elements from the base alloys, which may have a strengthening effect on the weld.^[23]

Tensile tests were carried out to investigate the strength of the arc welded dissimilar $Ti_3Al/In718$ joints with the Ni-Cu filler alloy. As listed in Table II, the average room-temperature tensile strength of the joints is 242 MPa, and the strength value at 873 K (600 °C) is 178 MPa, indicating that up to 73.6 pct of the room-temperature strength can be maintained.

During the welding process, the addition of the Ni-Cu filler alloy into the weld prevented the direct metallurgical reactions between the Ti_3Al -based alloy and the Ni-based superalloy and thus decreased the tendency of the formation of Ti-Ni brittle phases at the joint interface to a great extent. Furthermore, the Ni-Cu alloy has good ductility and deformation capacity, and its thermal expansion coefficient (about $13.5 \times 10^{-6}/K$) is between those of the two base alloys (about $10.7 \times 10^{-6}/K$ for Ti-24Al-15Nb-1Mo alloy and $17.0 \times 10^{-6}/K$ for In718 alloy). Therefore, the addition of the Ni-Cu alloy enhanced the fluidity of weld pool and was favorable to plastic deformation and residual stress relieving of the joints. Therefore, the mechanical properties of the $Ti_3Al/In718$ joints were improved under the present processing conditions. The possibility of dissimilar joining of Ti_3Al -based alloy and Ni-based superalloy by GTA welding has been verified.

All the samples fractured at the weld/ Ti_3Al interface in the tensile tests. Figure 6 shows the morphology of fractured surface of the $Ti_3Al/In718$ joint subjected to room-temperature tensile test. Obviously, the fracture displays a typical brittle rupture characterized by cleavage facets and river markings. Intermetallic compounds are commonly known as harmful phases with regard to mechanical properties.^[24] The weld/ Ti_3Al interface in this study contains lots of intermetallic phases such as Ti_2AlNb matrix dissolved with Ni and Cu, $Al(Cu, Ni)_2Ti$, and $(Cu, Ni)_2Ti$. They are hard but brittle and would lead to the brittle characteristic of the interface. Thus, the tensile properties of the joints in the present work are governed by the microstructure of the weld/ Ti_3Al interface. The composition analysis results of typical microstructures (labeled “1” and “2” in Figure 6) at the fractured surface are presented in Table III. It is easy to notice that the chemical composition of the regions marked by squares is almost identical to that of the light gray phase in layer “A” in Figure 3(a), signifying that the complex and brittle intermetallic phase of Ti_2AlNb matrix dissolved with Ni

Table III. Compositions of the Regions Marked by Squares in Fig. 6

Position	Composition (Atomic Percent)							Deduced Phase
	Ti	Ni	Cu	Al	Nb	Fe	Cr	
1	39.0	13.3	12.6	16.6	16.4	1.1	1.0	Ti_2AlNb matrix dissolved with Ni and Cu
2	44.9	9.7	10.8	17.0	16.2	0.8	0.6	

and Cu (“1” in Figure 3(a)) is the bonding weak link of the Ti₃Al/In718 joint. More research work should also be carried out in the future on this subject to improve the joint microstructures and to enhance the joint mechanical properties.^[25,27]

IV. CONCLUSIONS

1. In this study, a Ti₃Al-based alloy (Ti-24Al-15Nb-1Mo) and Inconel 718 superalloy were successfully welded using a Ni-Cu alloy as filler material by GTA welding technology and sound joints have been obtained.
2. The weld/Ti₃Al interface is composed of three transitional layers, where the typical intermetallic compounds include Ti₂AlNb matrix dissolved with Ni and Cu, Al(Cu, Ni)₂Ti and (Cu, Ni)₂Ti. Additionally, (Nb, Ti) and (Cu, Ni) solid solutions dissolved with several elements are also detectable. The phase constitutions of the fusion weld and In718/weld interface are mainly (Cu, Ni) solid solutions dissolved with two, three, or four elements of Ti, Nb, Fe, and Cr.
3. The weld exhibits higher microhardness than the two base materials. The average room-temperature tensile strength of the joints reaches 242 MPa, and up to 73.6 pct of the value can be maintained at 873 K (600 °C).
4. The fracture occurred at layer “A” of the weld/Ti₃Al interface, signifying that the complex and brittle intermetallic phase of Ti₂AlNb matrix dissolved with Ni and Cu is the bonding weak link of the Ti₃Al/In718 joint.

ACKNOWLEDGMENTS

This work was financially supported by the National Natural Science Foundation of China (No. 51405456).

REFERENCES

1. S. Djanarthany, J.C. Viala, and J. Bouix: *Mater. Chem. Phys.*, 2001, vol. 72, pp. 301–19.
2. S.J. Yang, S.W. Nam, and M. Hagiwara: *Intermetallics*, 2004, vol. 12, pp. 261–74.
3. H.P. Xiong, J.Y. Mao, B.Q. Chen, Q. Wang, S.B. Wu, and X.H. Li: *J. Mater. Eng.*, 2013, vol. 10, pp. 1–12 (in Chinese).
4. S.A. David, J.A. Horton, and G.M. Goodwin: *Weld J.*, 1990, vol. 69, pp. 133–40.
5. M.J. Cieslak, T.J. Headley, and W.A. Baeslack, III: *Metall. Trans. A*, 1990, vol. 21A, pp. 1273–86.
6. B. Liu, Y. Wu, Z.X. Zhou, Y.X. Cui, and D.H. Yang: *Mater. Sci. Technol.*, 1997, vol. 5, p. 45.
7. A.P. Wu, G.S. Zou, J.L. Ren, H.J. Zhang, G.Q. Wang, X. Liu, and M.R. Xie: *Intermetallics*, 2002, vol. 10, pp. 647–52.
8. Z.L. Lei, Z.J. Dong, Y.B. Chen, J. Zhang, and R.C. Zhu: *Mater. Des.*, 2013, vol. 46, pp. 151–56.
9. H.T. Zhang, P. He, J.C. Feng, and H.Q. Wu: *Mater. Sci. Eng., A*, 2006, vol. 425, pp. 255–59.
10. L.J. Tan, Z.K. Yao, W. Zhou, H.Z. Guo, and Y. Zhao: *Aerosp. Sci. Technol.*, 2010, vol. 14, pp. 302–06.
11. Z. Sun and R. Karppi: *J. Mater. Process Technol.*, 1996, vol. 59, pp. 257–67.
12. S. Chatterjee, T.A. Abinandanan, and K. Chattopadhyay: *J. Mater. Sci.*, 2006, vol. 41, pp. 643–52.
13. M. Velu and S. Bhat: *Mater. Des.*, 2013, vol. 47, pp. 793–809.
14. A.R. Miedema, F.R.D.E. Boer, R. Boom, and J.W.F. Dorleijn: *CALPHAD.*, 1977, vol. 1, pp. 353–59.
15. J.D. Keyzer, G. Cacciamani, N. Dupin, and P. Wollants: *CALPHAD.*, 2009, vol. 33, p. 109.
16. H.M. Li, D.Q. Sun, X.Y. Gu, P. Dong, and Z.P. Lv: *Mater. Des.*, 2013, vol. 50, pp. 342–50.
17. J.X. Cao, F. Bai, and Z.X. Li: *Mater. Sci. Eng. A*, 2006, vol. 424, pp. 47–52.
18. P. Villars, A. Prince, and H. Okamoto: *Handbook of Ternary Alloy Phase Diagrams*, ASM International, Materials Park, OH, 1995.
19. P. He, J.C. Feng, and H. Zhou: *Mater. Charact.*, 2005, vol. 54, pp. 338–46.
20. S.J. Lee, S.K. Wu, and R.Y. Lin: *Acta Mater.*, 1998, vol. 46, pp. 1283–95.
21. R.K. Shiue, S.K. Wu, and S.Y. Chen: *Acta Mater.*, 2003, vol. 51, pp. 1991–2004.
22. T. Tetsui: *Intermetallics*, 2001, vol. 9, pp. 253–60.
23. M. Kazunari, I. Yuki, M. Hirota, and M. Hiroyuki: *Scripta Mater.*, 2013, vol. 68, pp. 777–80.
24. M. Emamy, N. Nemati, and A. Heidarzadeh: *Mater. Sci. Eng. A*, 2010, vol. 527, pp. 2998–3004.
25. B.Q. Chen, H.P. Xiong, S.Q. Guo, X.J. Zhang, B.B. Sun, and S.Y. Tang: *J. Mater. Eng.*, 2014, vol. 4, pp. 13–17 (in Chinese).
26. B.Q. Chen, H.P. Xiong, B.B. Sun, S.Y. Tang, S.Q. Guo, and X.J. Zhang: *J. Mater. Sci. Technol.*, 2014, vol. 30, pp. 715–21.
27. B.Q. Chen, H.P. Xiong, B.B. Sun, S.Y. Tang, B.R. Du, and N. Li: *Prog. Nat. Sci.*, 2014, vol. 24, pp. 313–20.